Updated Performance and Operating Characteristics of a Novel Rotating Spool Compressor

International Compressor Engineering Conference at Purdue, July 11-14, 2014

Joe Orosz
Torad Engineering
Cumming, Georgia

Craig R. Bradshaw, PhD
Torad Engineering LLC
Cumming, Georgia

Greg Kemp
Torad Engineering LLC
Cumming, Georgia

Eckhard A. Groll, PhD
Ray W. Herrick Laboratories and Cooling Technologies Research Center
West Lafayette, Indiana

Updated Performance and Operating Characteristics of a Novel Rotating Spool Compressor

Joe OROSZ[1*], Craig R. BRADSHAW[2], Greg KEMP[3], Eckhard A. GROLL[4]

[1]Torad Engineering, 5192 Performance Drive
Cumming, GA 30040
Phone – (770-889-8400), Fax – (770-889-6900), E mail – joe.orosz@toradengineering.com

[2]Torad Engineering, 5192 Performance Drive
Cumming, GA 30040
Phone – (770-889-8400). Fax – (770-889-6900), E mail – craig.bradshaw@toradengineering.com

[3]Torad Engineering, 5192 Performance Drive
Cumming, GA 30040
Phone – (770-889-8400), Fax – (770-889-6900), E mail – greg.kemp@toradengineering.com

[4]Ray W. Herrick Laboratories, West Lafayette, IN 47907
Phone – (765-496-2201). Fax – (765-494-0787), E mail – groll@purdue.edu

* Corresponding Author

ABSTRACT

The basic mechanism of the novel rotary spool compressor has been described previously by Kemp et al. (2008, 2010). The device combines various aspects of rotary and reciprocating devices that are currently well understood. Due to increasing pressure in the global market for refrigerants with very low GWP levels extensive modeling was conducted to explore a spool compressor design for operation on medium pressure low GWP refrigerants in sizes applicable to the commercial air conditioning marker, specifically for application on air and water cooled chillers. The basis for a compressor design in this space is operation on R134a realizing that most low-GWP medium pressure gases are similar in nature to R134a from a compressor design point of view. A new compressor design with specific aspect ratio optimized for operation on R134a has been constructed and tested. The compressor was tested at a range of conditions suitable for evaluation in this application. The current compressor performance is comparable with today's screw compressors operating in this size range.

1. INTRODUCTION

The rotating spool compressor is a novel rotary compressor mechanism most similar to the sliding vane compressor. Primary differences are described by Kemp *et al*. (2008, 2010) and include three key differences from a sliding vane compressor, as shown in Figure 1.

- The vane is constrained by means of an eccentric cam allowing its distal end to be held in very close proximity to the housing bore while never contacting the bore.
- The rotor has affixed endplates that rotate with the central hub and vane forming a rotating spool.
- The use of dynamic sealing elements to minimize leakage between the suction and compression pockets as well as between the process pockets and the compressor containment.

The movement of the rotor is purely rotary with only the vane and tip seals performing any oscillating movement. The eccentric cam will force the movement of the vane to oscillate by twice the eccentricity during a single rotation. The tip seals will oscillate relative to the vane two times per rotation by an amount proportional to the ratio of diameters of the rotor to the housing bore (also known as the eccentricity ratio). The tip seal movement amount is roughly an order of magnitude smaller than the eccentricity and follows a sinusoidal path. Analytical details regarding the

geometry, including the mathematical expressions describing the chamber volumes, is presented in Bradshaw and Groll (2013).

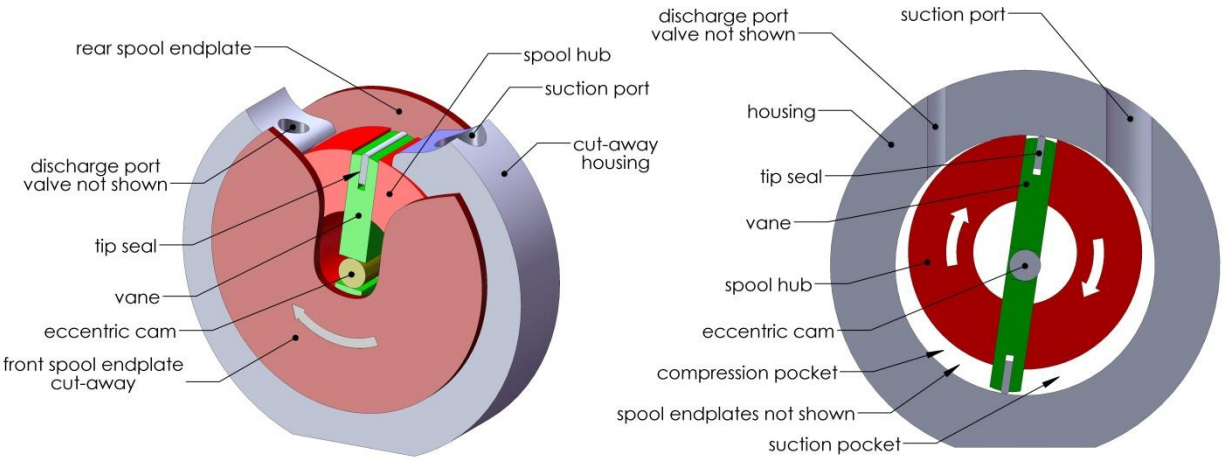

Figure 1: Cutaway view of rotating spool compressor mechanism with key components highlighted.

Since its introduction in 2008 the spool compressor has been improved and better understood. A comprehensive model was developed to deepen the understanding of the device holistically, as a system (Bradshaw and Groll, 2013). This holistic approach has allowed for better prediction of non-intuitive behavior of the spool compressor especially applied to applications and working fluids without experimental experience. The model includes 10 leak paths, 8 heat flow paths, port geometries, as well as oil solubility and frictional component sub-models.

Additionally, sub-components of the spool compressor have been studied in detail. Bradshaw (2013) presented a study on the analytical model developed to represent the tip seal in the spool compressor. The model was developed based on the tip seal dynamic model coupled with hydrodynamic lubrication theory. Kemp *et al.* (2012) presented iterations on the spool seal design and described the critical nature of the design of this component.

Bradshaw *et al.* (2016) recently presented the development of a loss analysis to describe the 5th generation spool compressor. This analysis utilized high-speed pressure measurements to determine the indicated, or flow, losses within the device. Coupled with analysis of the frictional losses a complete loss Pareto was generated. This analysis has resulted in a deep understanding of the location of potential improvements as well as an improved comprehensive modeling tool which accounts, more accurately, for the various frictional losses within the device. The resulting improvements using this analysis were also presented which showed a significant improvement in performance between the 5th and 6th generation compressor. These results echo the improved performance presented by Orosz *et al.* (2014).

This work presents an experimental characterization of a 141 kW (40 tonsR) prototype spool compressor for application to light-commercial air-conditioning. A custom-built hot-gas bypass load stand is described including an uncertainty analysis. The experimental performance data at two speeds is presented and discussed.

2. PERFORMANCE EVALUATION

A 141 kW (40 tonsR) R134a spool compressor was constructed to validate the modeling performed and presented by Bradshaw *et al.* (2016a). The compressor was mapped at two speeds with a range of suction pressures from 281.4 kPa (40.81 psia) to 497.5 kPa (72.2 psia) and a range of discharge pressures from 699.1 kPa (101.4 psia) to 1472.0 kPa (213.5 psia) utilizing R134a as the working fluid. This represents evaporating and condensing temperatures of -1.1 °C (30 °F) to 15.5 °C (60 °F) and 26.7 °C (80 °F) to 48.9 °C (120 °F), respectively. Intake gas superheat was fixed at 16.7 ºC (30 ºF) for all data points. These conditions represent a typical commercial air-conditioning application for both water and air cooled conditions.

2.2 Test Stand

Construction of a hot gas by-pass test stand was necessary to test the constructed prototype. This test stand needed accommodate the larger capacity compressor, up to 141 kW (40tonsR) of cooling. A schematic of this test stand is shown in Figure 2. The test stand includes the ability to separate and meter oil back into the compressor sump as well as into the intake for better simulation of actual system conditions. In addition, the test stand was designed to be ASHRAE 23.1 compliant and, where practical, includes redundant measurements on all critical functions including pressure, temperature and mass flow rate. Mass flow sensors are installed on the discharge as well as the intake of the compressor. The discharge mass flow meter is utilized to calculate the efficiencies because the gas is entering at a higher super heat with less risk for two-phase flow. The mass balance is considered acceptable at a level below 1.5%. Steady state is determined by calculating the total statistical variance of critical measurements over a 15 minute period. The test point is considered stable when the temperature variance is less than 0.2 K (0.4 R), pressure variances below 6.8 kPa (1 psi), speed variance is below 1 rpm, and mass flow rate variance is below 0.007 kg/sec (1 lb/min). The operating conditions of the compressor are controlled with software driven PID controllers which adjust the bypass valve, liquid line valve and condenser water flow controls. The power measurement is obtained with a rotary torque sensor and verified with the motor input power accounting for approximate motor efficiency.

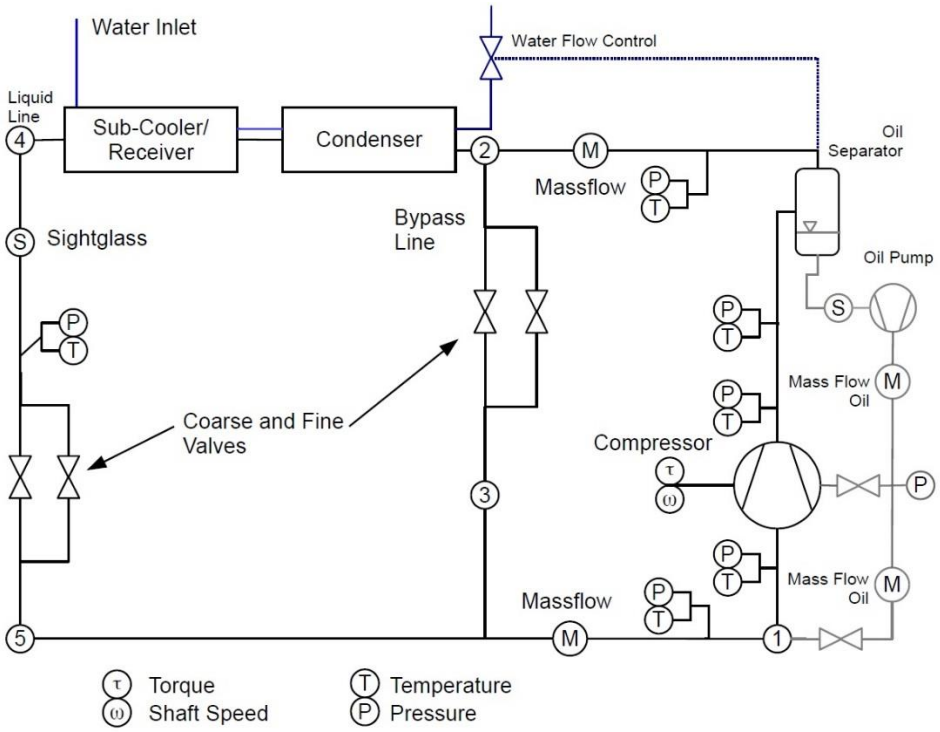

Figure 2: Schematic of 141 kW hot gas bypass test stand

Figure 3: Photo of 141 kW hot gas bypass test stand

2.2 Efficiency Definitions

Test data is collected to calculate the Volumetric Efficiency and Overall Isentropic Efficiency as a function of pressure ratio and speed. The volumetric efficiency was determined using Equation (1), where the theoretical volume flow was obtained based on speed measurements and the displacement volume:

$$\eta_{vol} = \frac{\dot{m}_{act} \cdot v_1}{\dot{V}_{th}} \quad (1)$$

where $\dot{m}_{act}$ and v_1 are the measured mass flow rate and specific volume, respectively. The overall isentropic efficiency is a frequently used measure for the first law efficiency of compressors by using an overall control volume, i.e., an evaluation by using the thermodynamic states at the compressor inlet and outlet. The overall isentropic efficiency is obtained based on Equation (2):

$$\eta_{is,o} = \frac{\dot{m}_{act} \cdot (h_{2s} - h_1)}{\dot{W}_{shaft}} \quad (2)$$

where $\dot{W}_{shaft}$ is the shaft power input to the compressor mechanism only.

2.3 Shaft Power Adjustments

For an open drive prototype the true shaft power cannot be measured directly because of the power draw of the shaft seal. Similarly, for a hermetic compressor the motor inefficiencies need to be accounted for to obtain a true shaft power. The efficiency numbers presented here include the loses associated with the shaft seal, as a shaft seal map was unavailable. In the case of a hermetic application the shaft seal would be replaced with a hermetic motor and these loses would need to be accounted for.

2.4 Uncertainty Analysis

The uncertainties associated with the measurements collected from the load stand are presented in this section. These measurements include temperature, pressure, refrigerant mass flow, compressor speed and compressor torque. The absolute uncertainty is given in Table 1. As the uncertainty of the temperature measurements are defined by the following relationship,

$$\mu = (.15 + .002*T) \tag{3}$$

where T is the actual temperature measured, in °C. In Table 1 the accuracy stated for the suction and discharge temperature respectively are for the specific operating condition of 4.4 ºC (40 ºF) Saturated Suction, 37.8 ºC (100 ºF) Saturated Discharge and 16.7 ºC (30 ºF) Suction superheat. Using the absolute uncertainty, the propagation of uncertainty associated with the reported efficiency values is calculated used and uncertainty propagation analysis (Fox *et al.* 2004). The volumetric and overall isentropic efficiencies have average uncertainty values of 0.6% and 1%, respectively.

Table 1: Uncertainty of Experimentally Obtained Measurements

Measured Value	Manufacturer	Model Number	Accuracy
Suction Pressure	Setra	ASM1200P	± .05%
Discharge Pressure	Omega	PX01-C1	± .05%
Discharge Mass Flow	Micromotion	CMF100	± .35%
Compressor Speed	Encoder Products	702	± .01%
Shaft Torque	S Himmelstein	79061V	± .15%
Suction Temperature	Omega	PRTF-17-2-100	± .75%
Discharge Temperature	Omega	PRTF-17-2-100	± .54%

4. COMPRESSOR PERFORMANCE

The 141 kW (40 tonsR) rotary spool compressor was evaluated based on the above running conditions using refrigerant R134a. Figures 4 and Figure 5 represent the volumetric efficiency for speeds 900 rpm and 1300 rpm, respectively, plotted against the pressure ratio for various condensing temperatures. The data points shift to the right as the condensing temperatures increases due to the constant suction pressures. At 900 rpm and 26.7 ºC (80ºF), the volumetric efficiency degrades at a rate of approximately 2.5% per pressure ratio and increases with increasing condensing pressure. At a condensing pressure of 43.3 ºC (110ºF), the volumetric efficiency degrades at a rate of 3% per pressure ratio. At 48.9 ºC (120ºF), the volumetric efficiency line exhibits a slight increase in slope from the 43.3 ºC (110ºF) line to 3.5% volumetric loss per pressure ratio. From Figure 5, 1300 rpm, it can be seen that the slope of the volumetric efficiency degradation per pressure ratio is 3% for all condensing temperatures. The total loss of volumetric efficiency at 900 rpm for the range of 1.5 pressure ratios to 4.5 pressure ratios is 14.5%. At 1300 rpm this improves to 9% for the same range of pressure ratios.

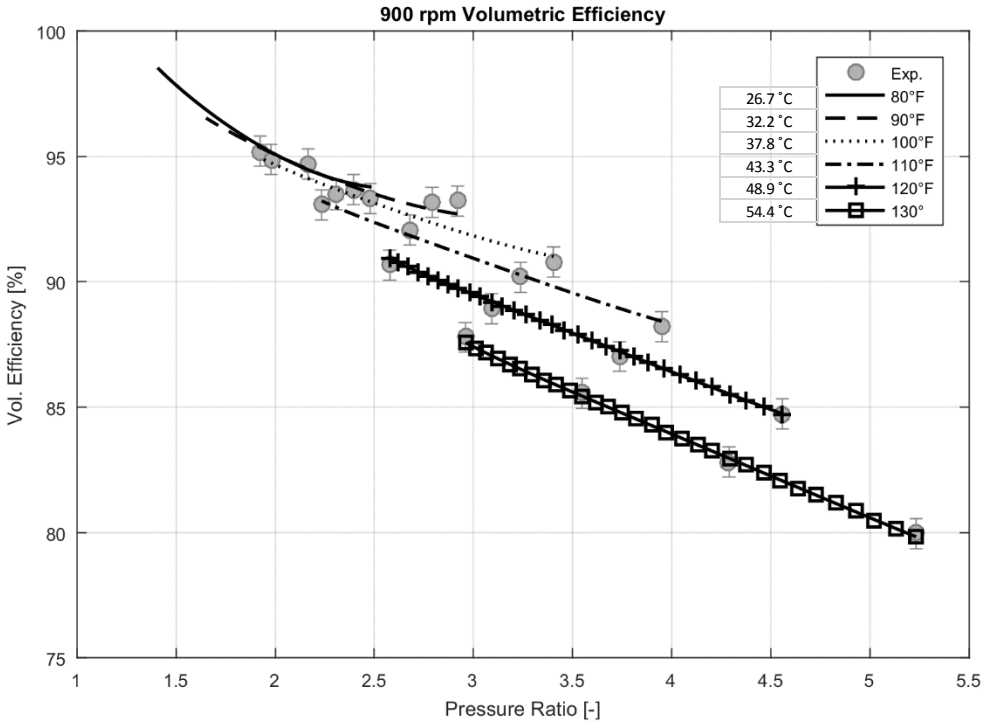

Figure 4: 141 kW spool compressor volumetric efficiency vs. pressure ratio at 900 rpm

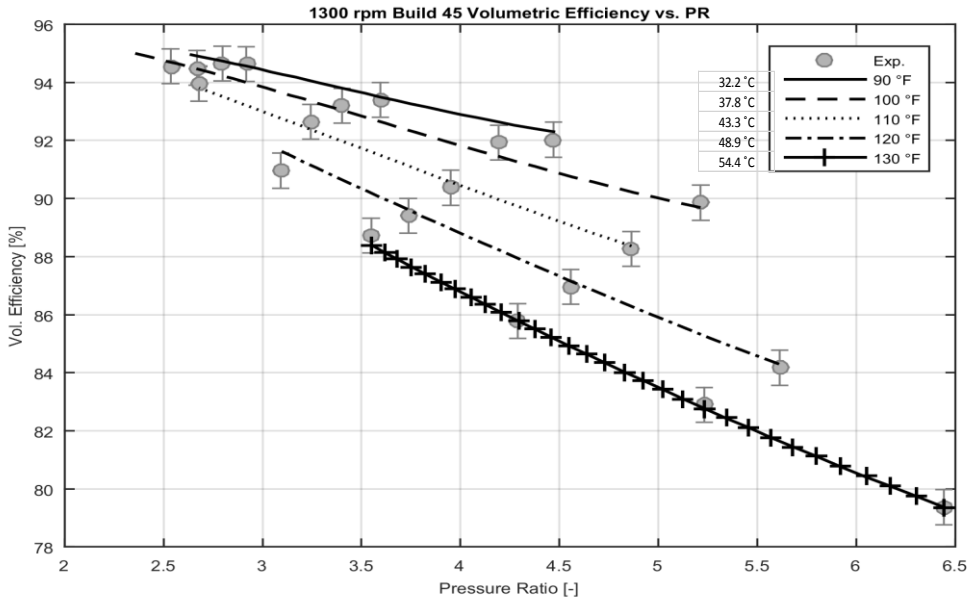

Figure 5: 141 kW (40 tonR) spool compressor volumetric efficiency vs. pressure ratio at 1300 rpm

Figures 6 and 7 present the overall isentropic efficiency at various pressure ratios at the two speeds, 900 and 1300 rpm, respectively. Looking at the 900 rpm curves in Figure 6, it can be seen that the spread between all condensing temperatures is in the range of 3.5% and the slope of the loss in overall isentropic efficiency per pressure ratio is 5.5%. Comparing that behavior to the 26.7ºC (80ºF) condensing line, it can be seen that this falls out of line with the balance of the data. Referring to Figure 8, it can be seen that the total shaft power required at 26.7ºC (80ºF) condensing is

quite small and as such the frictional loses become disproportionately high causing the overall isentropic efficiency to drop at a faster rate. This drop continues to increase as the pressure ratio gets lower. The 1300 rpm curve in Figure 7 shows that the range of overall isentropic efficiency has closed to 1.5% at pressure ratios less than 3.5 down from 2.5% at 900 rpm. The range of overall isentropic efficiency at pressure ratios greater than 3.5 increases to 4%. The slope of the loss of overall isentropic efficiency per pressure ratio has also improved from 5.5% to 3.8%. While the torque has increase slightly with increased speed the improvement in Volumetric performance has more than offset the incremental torque resulting in improved overall isentropic efficiency.

From Figures 6 and 7, it can be seen that the peak efficiency occurs at a pressure ratio of 2 in the 900 rpm case at 78%. The efficiency at 2.5 pressure ratios in the 1300 rpm case is 77% with the trend increasing with lower pressure ratio. Lower pressure ratio points were unattainable due to test stand limitations. The volumetric efficiency is approximately the same at both speeds and thus, the overall isentropic efficiency is being degraded by the increase in torque. Looking at a pressure ratio of 4 and a condensing temperature of 48.9ºC (120ºF) it can be seen that the overall isentropic is 67% at 900 rpm but improved to 70% at 1300 rpm. This is due to the improving slope of the volumetric efficiency with speed.

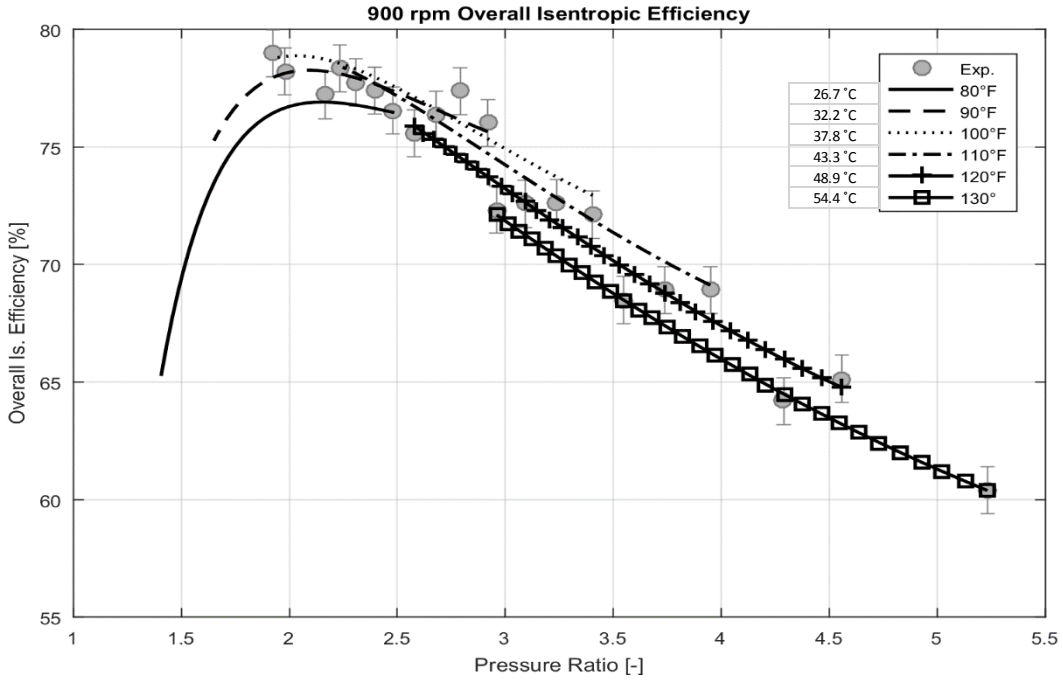

Figure 6: 141 kW spool compressor overall isentropic efficiency ($\eta_{is,0}$) vs. pressure ratio at 900 rpm

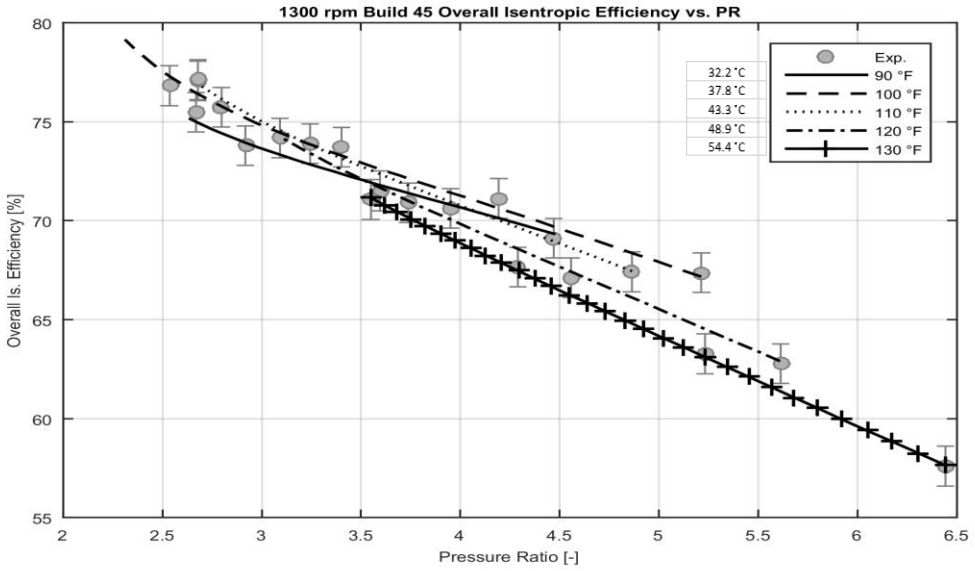

Figure 7: 141 kW spool compressor overall isentropic efficiency ($\eta_{is,0}$) vs. pressure ratio at1300 rpm

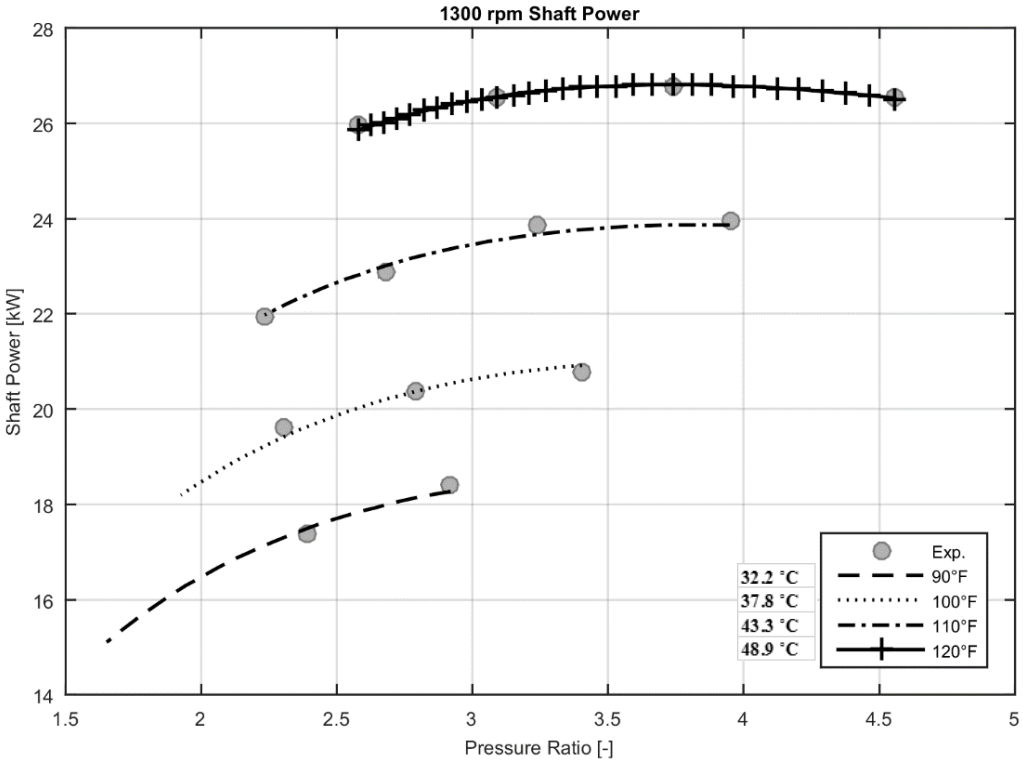

Figure 8: 141 kW spool compressor shaft power vs. pressure ratio

5. CONCLUSIONS

An experimental characterization of a prototype 141 kW (40 tonsR) R134a spool compressor is presented. This compressor design was based on the comprehensive modeling output presented in Bradshaw *et al.* (2016). A description of the custom-built hot-gas bypass test stand is included. The prototype compressor displayed good

efficiency across a wide operating range. Additionally, the spool compressor displayed a very good capability to perform at a wide range of shaft speeds, which could lead to efficient capacity control when integrated into a unit.

NOMENCLATURE

V_{Th}	Compressor Displacement, m^3/h	$\eta_{is,o}$,	Overall Isentropic Efficiency
$\dot{m}$	Mass flow, kg s-1	h	Specific Enthalpy, kJ kg-1
v	Specific Volume, m3 kg-1	P	Pressure of the gas, kPa
T	Temperature of the gas, K	$\dot{w}$	Work, kW
SSH	Intake Superheat, ºC	LSC	Liquid sub-cooling, ºC
Pr	Pressure Ratio	η_{vol}	Volumetric Efficiency
Rpm	Speed, Revolutions / min		

REFERENCES

Bradshaw, C.., Kemp, G., Orosz, J., Groll, E., 2012. A Comprehensive Model of a Novel Rotating Spool Compressor. In: Proceedings of the International Compressor Engineering Conference. Purdue University, West Lafayette, IN USA. No. 1142.

Bradshaw, C. R. and Groll, E. A. ,2013. A comprehensive model of a novel rotating spool compressor. International Journal of Refrigeration, 36(7):1974 – 1981. New Developments in Compressor Technology. Bradshaw, C.., Kemp, G., Orosz, J., Groll, E., 2014. Influence of Volumetric Displacement and Aspect Ratio on the Performance Metrics of the Rotating Spool Compressor. In: Proceedings of the International Compressor Engineering Conference. Purdue University, West Lafayette, IN USA. No. 1177.

Bradshaw, C.., Kemp, G., Orosz, J., Groll, E., 2014. Loss Analysis of Rotating Spool Compressor Based on High-Speed Pressure Measurements. Purdue University, West Lafayette, IN USA. No. 1178.

Bradshaw, C. R., Kemp, G., Orosz, J., and Groll, E. A., 2016. Development of a loss pareto for a rotating spool compressor using high-speed pressure measurements and friction analysis. Applied Thermal Engineering, 99:392–401.

Fox, R, McDonald, A., Pritchard, P., 2004. Introduction to Fluid Mechanics, 6th Edition, John Wiley and Sons.

Bradshaw, C.., Kemp, G., Orosz, J., Groll, E., 2016a. Design Methodology Improvements of a Rotating Spool Compressor using a Comprehensive Model. Purdue University, West Lafayette, IN USA. No. 1376.

Kemp, G., Elwood, L.., Groll, E., 2010. Evaluation of a Prototype Rotating Spool Compressor in Liquid Flooded Operation. In: Proceedings of the International Compressor Engineering Conference. Purdue University, West Lafayette, IN USA. No. 1389.

Kemp, G., Garrett, N., Groll, E., 2008. Novel Rotary Spool Compressor Design and Preliminary Prototype Performance. In: Proceedings of the International Compressor Engineering Conference. Purdue University, West Lafayette, IN USA. No. 1328.

Kemp, G., Orosz, J., Bradshaw, C., Groll, E., 2012. Spool Compressor Tip Seal Design Considerations and Testing. In: Proceedings of the International Compressor Engineering Conference. Purdue University, West Lafayette, IN USA. No. 1258.Kemp, G., Orosz, J., Bradshaw, C., Groll, E., 2012. Spool Seal Design and Testing for the Spool Compressor. In: Proceedings of the International Compressor Engineering Conference. Purdue University, West Lafayette, IN USA. No. 1259.

Orosz, J., Kemp, G., Bradshaw, C., Groll, E., 2012. Performance and Operating Characteristics of a Novel Rotating Spoll Compressor.

Orosz, J., Kemp, G., Bradshaw, C. R., and Groll, E. A. (2014). An update on the performance and operating characteristics of a novel rotating spool compressor. In International Compressor Engineering Conference at Purdue University, number 1378.